



# Constitutive expression of the global regulator AbrB restores the growth defect of a genome-reduced *Bacillus subtilis* strain and improves its metabolite production

Yamamoto, Junya ; Chumsakul, Onuma ; Toya, Yoshihiro ; Morimoto, Takuya ; Liu, Shenghao ; Masuda, Kenta ; Kageyama, Yasushi ; Hirasawa, Takash...

---

(Citation)

DNA Research, 29(3):dsac015

(Issue Date)

2022-06

(Resource Type)

journal article

(Version)

Version of Record

(Rights)

© The Author(s) 2022. Published by Oxford University Press on behalf of Kazusa DNA Research Institute.

This is an Open Access article distributed under the terms of the Creative Commons Attribution License (<https://creativecommons.org/licenses/by/4.0/>), which permits...

(URL)

<https://hdl.handle.net/20.500.14094/90009321>



Research Article

# Constitutive expression of the global regulator AbrB restores the growth defect of a genome-reduced *Bacillus subtilis* strain and improves its metabolite production

Junya Yamamoto<sup>1,†</sup>, Onuma Chumsakul<sup>2,†</sup>, Yoshihiro Toya<sup>3</sup>,  
Takuya Morimoto<sup>4</sup>, Shenghao Liu<sup>4</sup>, Kenta Masuda<sup>4</sup>, Yasushi Kageyama<sup>4</sup>,  
Takashi Hirasawa<sup>5</sup>, Fumio Matsuda<sup>3</sup>, Naotake Ogasawara<sup>2</sup>,  
Hiroshi Shimizu<sup>3</sup>, Ken-ichi Yoshida<sup>1</sup>, Taku Oshima<sup>6</sup>, and Shu Ishikawa<sup>1,\*</sup>

<sup>1</sup>Graduate School of Science, Technology and Innovation, Kobe University, Nada, Kobe 657-8501, Japan, <sup>2</sup>Graduate School of Biological Sciences, Nara Institute of Science and Technology, Ikoma, Nara 630-0192, Japan,

<sup>3</sup>Department of Bioinformatic Engineering, Graduate School of Information Science and Technology, Osaka University, Suita, Osaka 565-0871, Japan, <sup>4</sup>Biological Science Laboratories, Kao Corporation, Akabane, Tochigi 321-3497, Japan, <sup>5</sup>School of Life Science and Technology, Tokyo Institute of Technology, Yokohama, Kanagawa 226-8501, Japan, and <sup>6</sup>Department of Biotechnology, Toyama Prefectural University, Imizu, Toyama 939-0398, Japan

\*To whom correspondence should be addressed. Tel./Fax: +81-78-803-5907. Email: shu@people.kobe-u.ac.jp

<sup>†</sup>These authors contributed equally to this work.

Received 6 November 2021; Editorial decision 15 May 2022; Accepted 19 May 2022

## Abstract

Partial bacterial genome reduction by genome engineering can improve the productivity of various metabolites, possibly via deletion of non-essential genome regions involved in undesirable metabolic pathways competing with pathways for the desired end products. However, such reduction may cause growth defects. Genome reduction of *Bacillus subtilis* MGB874 increases the productivity of cellulases and proteases but reduces their growth rate. Here, we show that this growth defect could be restored by silencing redundant or less important genes affecting exponential growth by manipulating the global transcription factor AbrB. Comparative transcriptome analysis revealed that AbrB-regulated genes were upregulated and those involved in central metabolic pathway and synthetic pathways of amino acids and purine/pyrimidine nucleotides were downregulated in MGB874 compared with the wild-type strain, which we speculated were the cause of the growth defects. By constitutively expressing high levels of AbrB, AbrB regulon genes were repressed, while glycolytic flux increased, thereby restoring the growth rate to wild-type levels. This manipulation also enhanced the productivity of metabolites including  $\gamma$ -polylutamic acid. This study provides the first evidence that undesired features induced by genome reduction can be relieved, at least partly, by manipulating a global transcription regulation system. A similar strategy could be applied to other genome engineering-based challenges aiming toward efficient material production in bacteria.

**Key words:** silencing, AbrB, global regulator, genome reduction, *Bacillus subtilis*

## 1. Introduction

Notable progress in systematic genome reduction by genome engineering (hereafter referred to as ‘genome reduction’) has been achieved in the model bacteria *Bacillus subtilis* and *Escherichia coli* for nearly two decades.<sup>1</sup> Because deleting large non-essential parts of genomes may remove competing and unwanted metabolic pathways that divert cell resources from the production of desired end products, such genome-reduced strains may have increased capacity for the production of desired metabolites and reduced impact of cellular burden, along with greater robustness and increased energy efficiency for a wide range of applications.<sup>2</sup> Indeed, several genome-reduced strains that have beneficial traits compared with their parental wild-type strains have been reported to date. For example, *B. subtilis* MGB874 showed improved production of secreted heterologous enzymes.<sup>3,4</sup> The production and secretion of *Staphylococcus aureus* antigens and lantibiotics that are difficult to express in other *B. subtilis* strains was achieved in the MiniBacillus strain GP10.<sup>5,6</sup> *Escherichia coli* DGF-298 showed better growth fitness and cell yields compared with those of the wild-type strain.<sup>7</sup>

However, genome reduction can also result in undesirable phenotypes such as growth defects<sup>8</sup> and aberrant cellular and nucleoid morphologies.<sup>9</sup> In the case of *B. subtilis* GP10, despite acquiring a trait for effective production, genome reduction results in decreased growth rate compared with that of the parental strain, even when grown in a rich medium, likely resulting from deletion of a ribosomal RNA gene.<sup>10,11</sup> In the genome reduction process of *E. coli* DGF-298, further deletion became difficult due to the problems in growth fitness and cell yield when the genome size approached 3 Mb, and construction of the DGF-298 strain required restoration of the *proVWX* hyperosmolarity regulator genes to maintain growth.<sup>7</sup> Thus, given that large/extensive genome reduction is associated with tradeoffs of undesirable phenotypes caused by gene deletion and changes in gene expression, there is likely an optimal reduction size for creating beneficial strains, which can be used for research and technology development.

In the case of the *B. subtilis* MGB874 strain, deletion of 0.87 Mb (20%) of the genome reduced the growth rate, especially in minimal medium.<sup>3</sup> In our preliminary transcriptome experiments, we found that AbrB-regulated genes were upregulated in strain MGB874 compared with those in the wild-type strain. AbrB is a global regulator that directly represses ~250 genes involved in cell differentiation into several cell types with distinct phenotypes such as sporulating, genetically competent, motile, extracellular matrix-producing, and degradative enzyme-producing cells, which form multicellular communities known as biofilms on an agar plate or on a liquid surface (Fig. 1A).<sup>12–14</sup> Cell differentiation is also observed in liquid culture in shaking flasks where the cells are kept dispersed.<sup>15</sup> This process is initiated by a decrease in AbrB expression via transcriptional repression caused by binding of phosphorylated Spo0A to the promoter region immediately downstream of the transcriptional start site of *abrB* (Fig. 1B).<sup>16</sup> Interestingly, in the *spo0A12* mutant strain, in which the 62nd codon of the *spo0A* gene is replaced by an amber mutation,<sup>17</sup> AbrB is expressed at 2- to 4-fold higher levels than that in the wild-type strain, which was consistently found in various minimal media and accompanied by a significantly increased growth rate, whereas deletion of *abrB* decreased the growth rate compared with that of the wild-type strain.<sup>18</sup> These findings suggest that, even in exponentially growing wild-type cells cultured in minimal medium, transcription of *abrB* is only partially repressed by Spo0A to induce a large number of AbrB-regulated genes, which would induce

metabolic pathways that compete for cellular resources required in the pathway for the production of a desired end product (Fig. 1), consequently decreasing the growth rate. Therefore, further growth reduction would occur in the absence of AbrB, which fully induces the AbrB-regulated genes, and absence of the repressor Spo0A would increase the growth rate relative to that of the wild-type because high AbrB expression levels strictly repress AbrB-regulated genes. Considering these findings and presumptions, we hypothesized that constitutive expression of AbrB at a high level may rescue the reduced proliferation rate of MGB874.

Modulation of global transcription factors that could change global gene expression patterns offers a potential novel genome-wide approach to improve growth rate and material production in genome-engineered cells. In *E. coli*, overexpression of Lrp increases L-valine production<sup>19</sup> and overexpression of modified H-NS improves acid tolerance.<sup>20</sup> Lrp and H-NS are nucleoid-associated proteins,<sup>21</sup> and our previous chromatin immunoprecipitation (ChIP)-chip and genome footprinting by high-throughput sequencing results suggest that AbrB binds to hundreds of sites on the *B. subtilis* genome and represses over 100 genes, similar to H-NS in *E. coli*.<sup>13,14</sup> Exploration and visualization of single-molecule tracking data revealed the highly dynamic binding of AbrB throughout the genome, forming one or two regions of high-intensity binding on the nucleoids, similar to those of H-NS,<sup>22,23</sup> which preferentially binds adenine and thymine-rich DNA to repress the expression of numerous genes.<sup>24</sup> These data suggest that AbrB may silence a large number of genes simultaneously.

In this study, we investigated the effects of the constitutive high expression of *abrB* on the growth rate of the wild-type and MGB874 strains in minimal medium, along with its effects on the productivity of  $\gamma$ -polyglutamic acid ( $\gamma$ -PGA) and cellulase. This study provides the first demonstration that the problems induced by genome reduction can be solved, at least partly, by changing the expression level of a global transcription regulation system.

## 2. Materials and methods

### 2.1. Strain construction

The strains and plasmids used in this study are listed in [Supplementary Table S1](#). The primers used for strain construction and verification are listed in [Supplementary Table S2](#). The OA105 strain, in which two prophages (SP $\beta$  and PBSX), seven prophage-like regions (pro1 to pro7), and genes for the synthesis of plipastatin and bacillaene (*pps* and *pks*, respectively) were deleted, was used as the wild-type strain for most experiments instead of the parental 168 strain to avoid the interference of prophage induction and antibiotic production.<sup>25</sup> Strains A-001 and A-024 were derived from strains 168 and MGB874 with restored tryptophan autotrophy, respectively. Construction of the strains and plasmids is detailed in the [Supplementary Data](#).

### 2.2. Culture conditions

The strains were cultured in minimal medium buffered with MOPS (3-(*N*-morpholino)-propanesulfonic acid) (MMOPS medium, also referred to simply as minimal medium in this article) as previously described with the following modifications.<sup>25</sup> First, glycerol stock was inoculated onto MYC solid medium [MMOPS medium supplemented with 10 g l<sup>-1</sup> glucose, 1 g l<sup>-1</sup> Bacto yeast extract (Difco Laboratories, Franklin Lakes, NJ, USA), and 0.4 g l<sup>-1</sup> casamino acids (Difco Laboratories)] and cultured at 37°C for 10 h. For

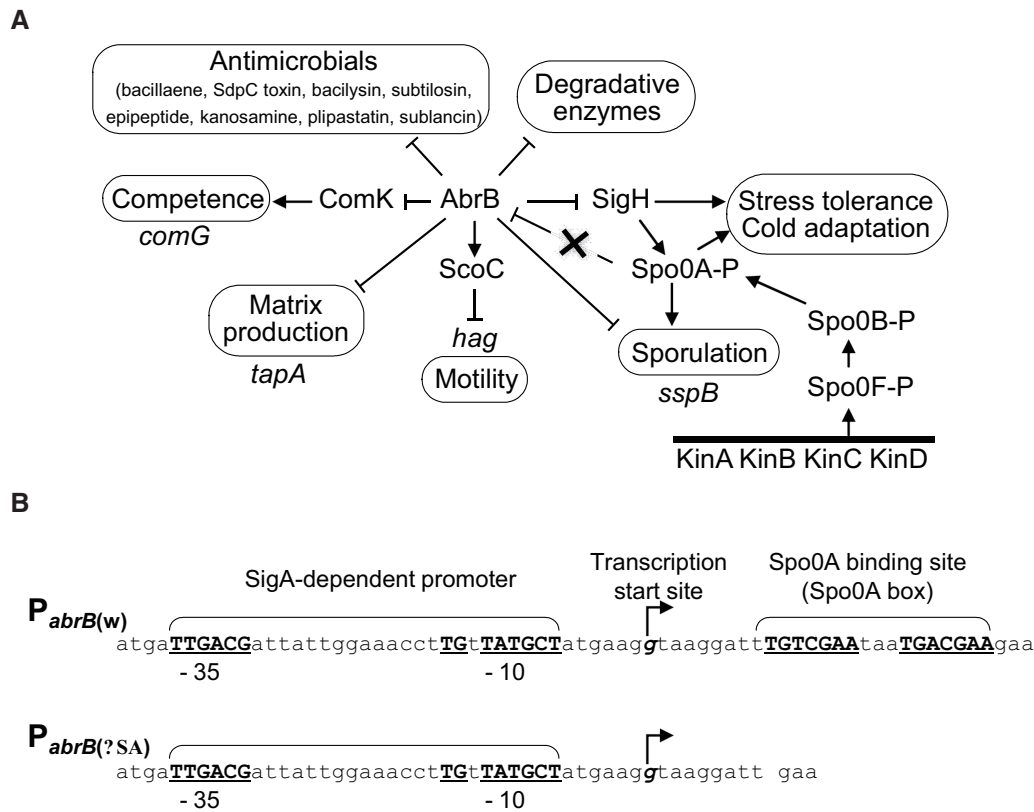


**Figure 1.** Transcriptional network centered on AbrB and the  $P_{abrB(\Delta SA)}$  mutation. (A) Spo0A is phosphorylated via a multicomponent system called phosphorelay from at least four sensor kinases (KinA, KinB, KinC, and KinD) to two phosphotransferases (Spo0F and Spo0B). Global gene silencing by AbrB is released by a decrease in the level of AbrB due to transcriptional repression of *abrB* caused by binding of Spo0A-P to the Spo0A box at the *abrB* promoter region.  $P_{abrB(\Delta SA)}$ , an *abrB* promoter in which the Spo0A-binding sequence was deleted, is relieved from Spo0A-P-mediated repression without losing Spo0A function (indicated by a cross). Genes whose promoters used in this study are also indicated. (B) Sequences and features of the *abrB* promoter regions of the wild-type [ $P_{abrB(w)}$ ] and the Spo0A box-deleted mutant [ $P_{abrB(\Delta SA)}$ ].

preculture, cells were collected from colonies, inoculated into 30 ml of MMOPS medium containing  $10 \text{ g l}^{-1}$  glucose to obtain an optical density at 600 nm ( $\text{OD}_{600}$ ) of 0.01, and cultured at  $37^\circ\text{C}$  with shaking at 200 rpm in a 300-ml flask until the  $\text{OD}_{600}$  reached 1–2. For the main culture, this preculture was inoculated in 50 ml of MMOPS medium with 10, 20, or  $50 \text{ g l}^{-1}$  glucose to obtain an  $\text{OD}_{600}$  below 0.1, followed by culturing at  $37^\circ\text{C}$  with shaking at 200 rpm in a 500-ml flask. Unless otherwise noted,  $40 \text{ g l}^{-1}$   $\text{CaCO}_3$ , which is soluble at acidic pH but hardly soluble at neutral pH, was added to maintain the culture medium at a neutral pH.

### 2.3. $\beta$ -Galactosidase assay

To monitor  $\beta$ -galactosidase activity in liquid medium, the cells were grown in MMOPS medium containing  $20 \text{ g l}^{-1}$  glucose at  $37^\circ\text{C}$  with shaking, and 1 ml of culture was collected every 2 h to determine  $\beta$ -galactosidase activity, as previously described.<sup>26</sup> To accurately measure galactosidase activity,  $\text{CaCO}_3$  was not added to the medium. Therefore, the pH decreased during the stationary phase, and the activity during the stationary phase was not measured.

### 2.4. Growth and fluorescence measurements for long-term culture

For long-term culture using a microplate reader (BioTek, Winooski, VT, USA), MMOPS medium was used as described above but with

the following modification. For the preculture, MYC solid medium containing  $5 \text{ g l}^{-1}$  glucose was used. Because  $\text{CaCO}_3$  could not be added to measure the  $\text{OD}_{600}$  and fluorescence in a microplate reader, MMOPS medium containing  $20 \text{ g l}^{-1}$  glucose was used to maintain a neutral pH under these conditions. For the main culture, the preculture was inoculated to obtain an  $\text{OD}_{600}$  of 0.02 in 0.15 ml of MMOPS medium, followed by culture in a 96-well black/clear bottom plate (Thermo Fisher Scientific, Waltham, MA, USA) at  $37^\circ\text{C}$  with double-orbital shaking at the ‘Fast’ speed setting, and  $\text{OD}_{600}$  (and fluorescence, if necessary) readings were taken every 0.5 h over a 45-h period. To ensure aeration and prevent the drying of culture media during long-term culture, the microplate was sealed with an oxygen-permeable transparent membrane (0.3-mm thick polydimethylsiloxane-non-coating sheet, VECCELL Inc. Fukuoka, Japan).

### 2.5. Flow cytometric analysis

Flow cytometric analysis was carried out as described previously with the following modifications.<sup>27</sup> Cells cultured in MMOPS medium in a microplate as described above were fixed with 4% (v/v) formaldehyde at  $25^\circ\text{C}$  for 30 min, washed once in a buffer (10 mM Tris-HCl [pH 8.0], 1 mM EDTA, 200 mM KCl, and 5% [v/v] glycerol) suspended in phosphate-buffered saline (1 mM  $\text{KH}_2\text{PO}_4$ , 3 mM  $\text{Na}_2\text{HPO}_4$ , and 155 mM NaCl), and analyzed by flow cytometry using CytoFlexS (Beckman Coulter, Brea, CA, USA) without

sonication. Data analysis was performed using the CytoExpert software bundle. Green fluorescence was detected using a fluorescein isothiocyanate channel (525/40 BP) with an excitation beam at 488 nm. A total of 100,000 events were detected at a rate of  $<1,500$  events  $s^{-1}$ .

## 2.6. Transcriptome analysis

For transcriptome and metabolic analyses, MMOPS medium containing  $10\text{ g l}^{-1}$  glucose was used, and  $40\text{ g l}^{-1}$   $\text{CaCO}_3$  was added to maintain the neutral pH of the culture medium. However,  $\text{CaCO}_3$  degrades RNA during the extraction process. Because we found that high-purity ultrafine  $\text{CaCO}_3$  particles ( $1\text{--}50\text{ }\mu\text{m}$ , Shiraishi Kogyo Kaisha, Ltd., Osaka, Japan) were resolved by mixing with EDTA, we used the ultrafine  $\text{CaCO}_3$  particles for RNA extraction, which were first resolved by mixing with an equal volume of  $0.5\text{ M}$  EDTA (pH 8.0) for 3 min at room temperature. The cells were then collected by centrifugation at  $5,000\times g$  for 3 min, resuspended in a solution containing RNeasy Protect Bacteria Reagent (QIAGEN, Hilden, Germany), and  $0.5\text{ M}$  EDTA at a 2:1 ratio, and incubated for 5 min at  $25^\circ\text{C}$ . Cells were pelleted at  $15,000\times g$  for 1 min and stored at  $-80^\circ\text{C}$  until use. To measure the  $\text{OD}_{600}$ , cells and the  $\text{CaCO}_3$  suspension were mixed with five times the volume of HE buffer ( $0.1\text{ M}$  EDTA,  $0.1\text{ M}$  HEPES (4-(2-hydroxyethyl)-1-piperazineethanesulfonic acid), and pH 7.0) to resolve the ultrafine  $\text{CaCO}_3$  particles in advance.

RNA extraction, synthesis of complementary DNA, terminal labeling, and hybridization with the oligonucleotide tiling chip were all performed according to the Affymetrix instruction manual, as previously reported.<sup>28</sup> For transcriptome analysis, custom-designed Affymetrix GeneChips were used. Hybridization signal data, background correction, data normalization, and determination of expression levels of individual genes were all performed with the In Silico Molecular Cloning program, array edition (In Silico Biology), as previously described<sup>29</sup> with small modifications. In this study, relative signal intensities were calculated by subtracting the signal intensities of mismatched probes from those of perfectly matched probes and then adjusted to confer a signal average of 500 in each experiment. Raw data (CEL format) from the present transcriptome have been deposited in the ArrayExpress database under accession number E-MTAB-11245. Functional categories of genes involved in the central metabolism pathway (CMP) were assigned according to the SubtiWiki database.<sup>30</sup> The AbrB regulon includes seven transcriptional units that are known to be activated by AbrB, although the molecular mechanism is not clear; thus, only genes that are directly repressed by AbrB as listed in the SubtiWiki database (i.e. AbrB-regulated genes) were analyzed in this study. Differences in overall transcriptional changes in the CMP and AbrB-regulated genes, along with that in the genes involved in the biosynthesis of amino acids and purine/pyrimidine nucleotides were evaluated using a one-sided Mann–Whitney U-test with  $P$ -values  $< 0.05$  considered statistically significant (Supplementary Table S3). Genes classified into both CMP-related genes and AbrB-related genes were excluded from this analysis. The  $P$ -values are shown in box and whisker plots. To extract differentially expressed (DE) genes between MGB874 and OA191 and to conduct functional enrichment analysis, the Kyoto Encyclopedia of Genes and Genomes pathway for *B. subtilis* 168<sup>31</sup> and NetworkAnalyst tool were used.<sup>32</sup> Our normalized data were  $\log_2$ -transformed, processed by the *limma* program,<sup>33</sup> and visualized as a volcano plot; genes with  $\log_2$ -fold change  $\geq 1$  (upregulated) or  $\leq -1$  (downregulated) and  $P < 0.05$  were considered to be DE genes

(Supplementary Table S3). Differentially up- and downregulated genes were also evaluated at a cutoff value of 1.5-fold change which detected a similar number of DE genes detected by the volcano plot analysis (Supplementary Table S3).

## 2.7. Measurement of extracellular glucose and metabolites

The glucose concentration in the culture supernatants was measured using an enzyme electrode glucose sensor (BF-5; Oji Scientific Instruments, Hyogo, Japan). Acetate, acetoin, and succinate concentrations in the culture supernatants were measured using a high-performance liquid chromatography system (Shimadzu, Kyoto, Japan) equipped with an ultraviolet–visible detector (210 nm) with TSKgel OApak-A and TSKgel OApak-P columns (Tosoh, Tokyo, Japan). The detailed method is described elsewhere.<sup>34</sup> The specific rates of glucose consumption and acetate formation are defined as follows:

$$\begin{aligned} d[\text{glucose}]/dt &= -vX \\ d[\text{acetate}]/dt &= \rho X \end{aligned}$$

where  $X$  represents the biomass concentration [g-dry cell weight (DCW)  $\text{l}^{-1}$ ], and  $v$  and  $\rho$  ( $\text{mmol g-DCW}^{-1} \text{ h}^{-1}$ ) are calculated as the slopes of the regression lines between the integrated biomass concentration (g-DCW  $\text{l}^{-1} \text{ h}$ ) and glucose or acetate concentration ( $\text{mmol l}^{-1}$ ).<sup>35</sup>

## 2.8. Measurement of mass isotopomer distributions of proteinogenic amino acids

During the exponential phase (7.5–8 h), an appropriate amount of culture [ $\text{OD}_{600} \times \text{culture volume (ml)} = 8$ ] was collected via centrifugation. The cells were washed with 2 ml of  $0.2\text{ mol l}^{-1}$  HCl to remove the  $\text{CaCO}_3$  and then further washed with 2 ml saline. The cells were hydrolyzed with 2 ml of  $6\text{ mol l}^{-1}$  HCl at  $105^\circ\text{C}$  for 18 h. The samples were filtered through a Cosmonice filter W ( $0.45\text{ }\mu\text{m}$ ; Nacalai Tesque, Kyoto, Japan), mixed with  $10\text{ }\mu\text{l}$  of  $600\text{ }\mu\text{M}$  cycloleucine, dried, and dissolved in  $50\text{ }\mu\text{l}$  acetonitrile. After adding  $50\text{ }\mu\text{l}$  of  $N$ -(*tert-tert*-butyldimethylsilyl)- $N$ -methyl-trifluoroacetamide containing 1% *tert*-butyldimethylchlorosilane, the samples were incubated at  $105^\circ\text{C}$  for 1 h for derivatization. mass isotopomer distributions (MIDs) of proteinogenic amino acids were measured using a gas chromatograph/mass spectrometer (Agilent 7890A GC and 5975C Mass Selective Detector; Agilent Technologies, Santa Clara, USA) with a DB-5MS+DG column (Agilent Technologies). The detailed method is described elsewhere.<sup>34</sup>

## 2.9. $^{13}\text{C}$ -Metabolic flux analysis

The CMP of *B. subtilis* was considered for flux estimation. An elementary metabolite unit framework was used to model the carbon atom transitions.<sup>36</sup> All reactions, carbon atom transitions in CMP, and carbon atom transitions from precursor metabolites to amino acids are listed in Supplementary Table S4. Effluxes were determined from the measured specific rates and precursor requirements for the biomass synthesis of *B. subtilis*.<sup>37</sup> The flux distribution was estimated to minimize the residual sum of squares between the measured and simulated MIDs of amino acids. Comparisons between measured and simulated MIDs are summarized in Supplementary Table S5. Goodness of fit was assessed using the chi-square test. The 95% confidence interval (CI) of each flux was calculated using a grid



search algorithm.<sup>38</sup> Calculations were performed using OpenMebius software<sup>39</sup> in MATLAB R2014a (Mathworks, Natick, MA, USA).

### 2.10. Analyses of $\gamma$ -PGA and cellulase production

Strains A-278 [A-024: *tufA-pgdS* (*spc*), *amyE::P<sub>rrmO</sub>-pgsBCAE* (*cat*),  $\Delta$ *pgsBCAE-pgdS*] and A-306 [A-278: *P<sub>abrB</sub>( $\Delta$ SA)* (*erm*)] were grown in MMOPS medium supplemented with 50 g l<sup>-1</sup> glucose and  $\gamma$ -PGA after 24 h of culture and analyzed as previously described.<sup>40</sup> For cellulase production, the recombinant plasmid pHYS237 encoding a cellulase gene from *Bacillus* sp. KSM-S237<sup>3</sup> was introduced into strains A-001 (168: *trp*+) and A-395 [A-001: *P<sub>abrB</sub>( $\Delta$ SA)*]. The transformants were cultured in 2xL-Mal medium (2% tryptone peptone, 1% yeast extract, 1% NaCl, 7.5% maltose hydrate, and 7.5  $\mu$ g ml<sup>-1</sup> MnSO<sub>4</sub>) supplemented with 15 mg l<sup>-1</sup> tetracycline for 72 h at 37°C, and cellulase activity in the culture medium was determined as previously described.<sup>41</sup> Differences were assessed with one-sided Student's *t*-tests, and *P*-values < 0.05 were considered statistically significant.

## 3. Results

### 3.1. Deletion of the Spo0A binding site at the *abrB* promoter rescues the reduced growth of the genome-reduced strain MGB874

To create cells that have a potential for effective production of useful products such as secreted proteins and  $\gamma$ -PGA, it is essential to identify and counter the cause of the slow proliferation of MGB874 cells. Our preliminary transcriptome experiments revealed that the expression of AbrB-regulated genes was upregulated compared with that in the wild-type when grown in the minimal medium containing glucose and ammonium as the sole carbon and the nitrogen sources, respectively. We assumed that the gene repression by AbrB was partially deregulated in MGB874 during the process of genome reduction and the upregulated AbrB-regulated genes (Fig. 1A) reduced the growth rate. Thus, we expected that constitutive expression of AbrB at high levels, as in the *spo0A*-null mutant,<sup>18</sup> may rescue the slow-growth phenotype. Contrary to this expectation, *spo0A* deletion did not restore the slow-growth phenotype but rather showed an additional negative phenotype of a long lag time from inoculation to exponential growth in the minimal medium containing 20 g l<sup>-1</sup> glucose (Supplementary Fig. S1). A deletion mutant of *sigH*, whose product activates *spo0A* transcription (Fig. 1A), also showed a similar long-lag phenotype. These results indicated that *spo0A* and *sigH* play important roles in the growth of MGB874 in minimal medium. SigH is required for the survival of *B. subtilis* in alkaline or acidic medium and for growth in ethanol-containing medium,<sup>42</sup> and induction of Spo0A during exponential growth at 20°C is essential for stationary-phase viability in minimal medium (Fig. 1A).<sup>43</sup> Thus, SigH and Spo0A are necessary for adaptation to various stresses and may also play an important role in growth in minimal medium with limited nutrient sources. Accordingly, to increase the growth rate of MGB874, we considered that the relief of AbrB expression from the Spo0A-mediated repression without the loss of other Spo0A functions was required. To this end, we designed a promoter in which the Spo0A binding sequence, designated the Spo0A box, was deleted from the *abrB* promoter region [*P<sub>abrB</sub>( $\Delta$ SA)* mutation; Fig. 1B]. As expected, the growth rate of the MGB874 strain harboring the *P<sub>abrB</sub>( $\Delta$ SA)* mutation was restored to the level of the parental wild-type strain OA105 (Fig. 2).

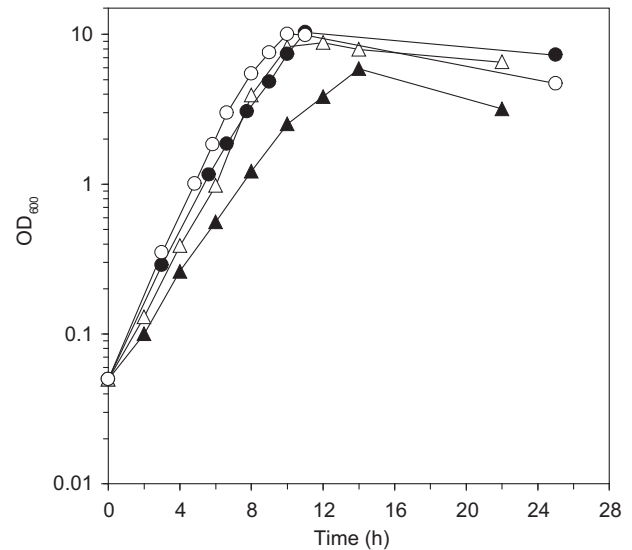


**Figure 2.** Growth of the wild-type and genome-reduced strain and their *P<sub>abrB</sub>( $\Delta$ SA)*-introduced derivatives. Growth curves of the wild-type strain (OA105, closed circles) and its *P<sub>abrB</sub>( $\Delta$ SA)* derivative (OA190, open circles), the genome-reduced strain (MGB874, closed triangles) and its *P<sub>abrB</sub>( $\Delta$ SA)* derivative (OA191, open triangles) grown in the minimal medium containing 10 g l<sup>-1</sup> glucose are shown.

### 3.2. *P<sub>abrB</sub>( $\Delta$ SA)* promoter is not repressed in minimal medium, thereby inhibiting the transcription of AbrB-regulated genes

We predicted that, in minimal medium, transcription of *abrB* would be partially repressed by Spo0A to induce a large number of AbrB-regulated genes, imposing a burden for exponentially growing cells (see Introduction for details). To confirm this prediction and check whether *P<sub>abrB</sub>( $\Delta$ SA)* was relieved from Spo0A repression to supply enough AbrB to inhibit the expression of AbrB-regulated genes, we monitored *abrB* promoter activity using LacZ assays in the minimal medium containing 20 g l<sup>-1</sup> glucose. The LacZ activity of the Spo0A box-deleted promoter fused with *lacZ* [*P<sub>abrB</sub>( $\Delta$ SA)-lacZ*] and the wild-type promoter fused with *lacZ* [*P<sub>abrB</sub>(W)-lacZ*] inserted in the *amyE* region on the chromosome was compared (Fig. 3A). *P<sub>abrB</sub>( $\Delta$ SA)-lacZ* was active in the exponential phase, whereas the activity of *P<sub>abrB</sub>(W)-lacZ* was repressed to a lower level. This result indicated that in minimal medium, Spo0A was activated to repress *P<sub>abrB</sub>(W)* in the exponential phase, whereas *P<sub>abrB</sub>( $\Delta$ SA)* was released from this repression.

To examine whether higher *abrB* transcription from *P<sub>abrB</sub>( $\Delta$ SA)* was sufficient to repress AbrB-regulated genes, the promoter activity of *sdpA*, which is repressed by direct AbrB binding and de-repressed in the absence of AbrB,<sup>13,14</sup> was compared using *P<sub>sdpA</sub>-lacZ* in the *P<sub>abrB</sub>( $\Delta$ SA)* mutant and wild-type strains (Fig. 3B). In the wild-type strain, although *P<sub>abrB</sub>(W)-lacZ* transcription was weakly induced during the exponential phase (at 10 h), *P<sub>sdpA</sub>-lacZ* transcription was induced during the exponential growth phase, indicating that *P<sub>sdpA</sub>-lacZ* was not repressed at this level of *abrB* expression. In contrast, in the *P<sub>abrB</sub>( $\Delta$ SA)* introduced strain [referred to as *P<sub>abrB</sub>( $\Delta$ SA)* strain], *abrB* showed a transcription level that was ~6.7 times higher than that of the wild-type, as detected from the slopes of the *P<sub>abrB</sub>-lacZ* values (Fig. 3A), and *P<sub>sdpA</sub>-lacZ* continued to be almost completely repressed even in the transition phase (Fig. 3B). These results clearly indicated that, in the *P<sub>abrB</sub>( $\Delta$ SA)* strain, AbrB is highly expressed at the level sufficient to strongly repress AbrB-regulated genes.

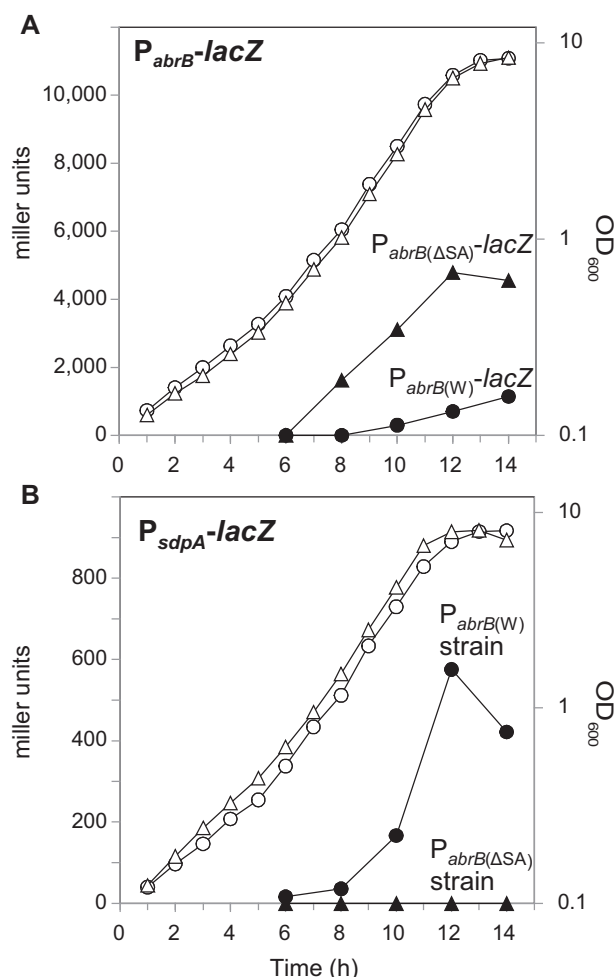


**Figure 3.** Effect of deletion of the Spo0A binding sequence at the *abrB* promoter. (A and B) LacZ assay of OA105-derived strains cultured in the minimal medium containing 20 g l<sup>-1</sup> glucose. (A) The expression of  $P_{abrB(W)}$ -lacZ (OA124, closed circles) and  $P_{abrB(\Delta SA)}$ -lacZ (OA125, closed triangles) and the growth of the OA124 (open circles) and OA125 (open triangles) strains carrying these promoter fusions are shown. (B) The expression of  $P_{sdpA}$ -lacZ in  $P_{abrB(W)}$  (OA131, closed circles) and  $P_{abrB(\Delta SA)}$  (OA137, closed triangles) and the growth of the OA131 (open circles) and OA137 (open triangles) strains carrying these promoter fusions are shown.

### 3.3. $P_{abrB(\Delta SA)}$ mutation represses genes involved in cell differentiation

During cultivation, small fractions of *B. subtilis* cells differentiate into the cells having different functions by expressing genes specific to each cell type.<sup>12–14</sup> We monitored this process using a green fluorescent protein (GFP) reporter assay for differentiation-related genes. To observe whether the  $P_{abrB(\Delta SA)}$  mutation in the MGB874 strain represses genes involved in cell differentiation in minimal medium, the promoter activities of *hag*, *tapA*, *sspB*, and *comG*, which are specifically expressed only in motile cells, matrix-producing cells, sporulating cells, and competent cells, respectively (Fig. 1), were measured with a microplate reader using GFP as a reporter and monitored for 45 h. All examined promoters were activated in MGB874 but at different times (Fig. 4A). In contrast, in the  $P_{abrB(\Delta SA)}$  strain, while  $P_{hag}$ -gfp exhibited weak activity, the activities of  $P_{tapA}$ -gfp,  $P_{sspB}$ -gfp, and  $P_{comG}$ -gfp were almost completely repressed at all examined time points (Fig. 4B).

Flow cytometric analysis using cells cultured under the same conditions was performed to examine the number of cells with such promoter activity in the population. Small portions of the population exhibited  $P_{tapA}$ -gfp,  $P_{sspB}$ -gfp, and  $P_{comG}$ -gfp activities, whereas cells with activated  $P_{hag}$ -gfp accounted for more than half of the population in MGB874 (Fig. 5). In contrast, in the  $P_{abrB(\Delta SA)}$ -introduced MGB874 strain, the cells showed a single peak, indicating that  $P_{abrB(\Delta SA)}$  almost completely suppressed differentiation, leading to a homogeneous, undifferentiated cell population.

### 3.4. $P_{abrB(\Delta SA)}$ mutation restores the decreased transcription of Central metabolic pathway genes in MGB874

We next examined how genome reduction and constitutive high expression of AbrB resulted in transcriptomic changes by performing a tiling array analysis. Figure 6 shows the transcription levels of all genes in exponentially growing cells in the minimal medium containing 10 g l<sup>-1</sup> glucose for OA105, MGB874, and their corresponding  $P_{abrB(\Delta SA)}$ -introduced strains.

The comparison of OA105 and MGB874 transcriptome profiles indicated that in the MGB874 strain, many AbrB-regulated genes were upregulated and many CMP-related genes were repressed (Fig. 6A). Although the overall transcriptional change of the AbrB-regulated genes was not statistically significant (Fig. 6E), 21% of the AbrB-regulated genes showed significant increase in expression level in MGB874 (Supplementary Table S3), as observed in preliminary transcriptome experiments. In contrast, the overall transcriptional reduction was statistically significant when comparing the repression of the CMP genes (Fig. 6F), and 21% of the CMP-related genes showed significant decrease in the expression level (Supplementary Table S3).

As described above, introduction of the  $P_{abrB(\Delta SA)}$  mutation into MGB874 restored the slow-growth phenotype to wild-type levels (Fig. 2A). This, in turn, resulted in a statistically significant difference in the overall transcription levels of AbrB-regulated and CMP genes (Fig. 6E and F); 54% of the AbrB-regulated genes were statistically downregulated and 21% of the CMP genes were statistically upregulated compared with those of the parental strain MGB874 (Supplementary Table S3 and Figs 6B, E, and F). As a result, overall transcription level of CMP genes was restored to a level that was both visually and statistically indistinguishable from that of the wild-type strain OA105 (Fig. 6C and F).

Gene set enrichment analysis of DE genes detected enrichment of various metabolic pathways ( $P = 3.0 \times 10^{-4}$ ). The dots for genes involved in glycolysis, pentose phosphate pathway (PPP), tricarboxylic acid (TCA) cycle, gluconeogenesis, and overflow metabolism in CMP are separately colored in the volcano plot between MGB874 and the  $P_{abrB(\Delta SA)}$ -introduced MGB874 strain (OA191) (Fig. 7C). Although the increase in the expression level of only glycolysis genes was statistically significant, most CMP genes were upregulated in the  $P_{abrB(\Delta SA)}$ -introduced strain (Figs 6B, 7A, and C).

### 3.5. $P_{abrB(\Delta SA)}$ mutation increases glycolytic flux in MGB874

To investigate how metabolism changes along with changes in transcription, we also performed <sup>13</sup>C-metabolic flux analysis simultaneously using the same culture medium that was used for the transcriptome analysis of the parent and  $P_{abrB(\Delta SA)}$ -introduced MGB874 strains. After flux optimizations, the residual sums of squares between measured and simulated MID were 65.5 and 87.1 for the MGB874 and  $P_{abrB(\Delta SA)}$  strains, respectively. It suggests that

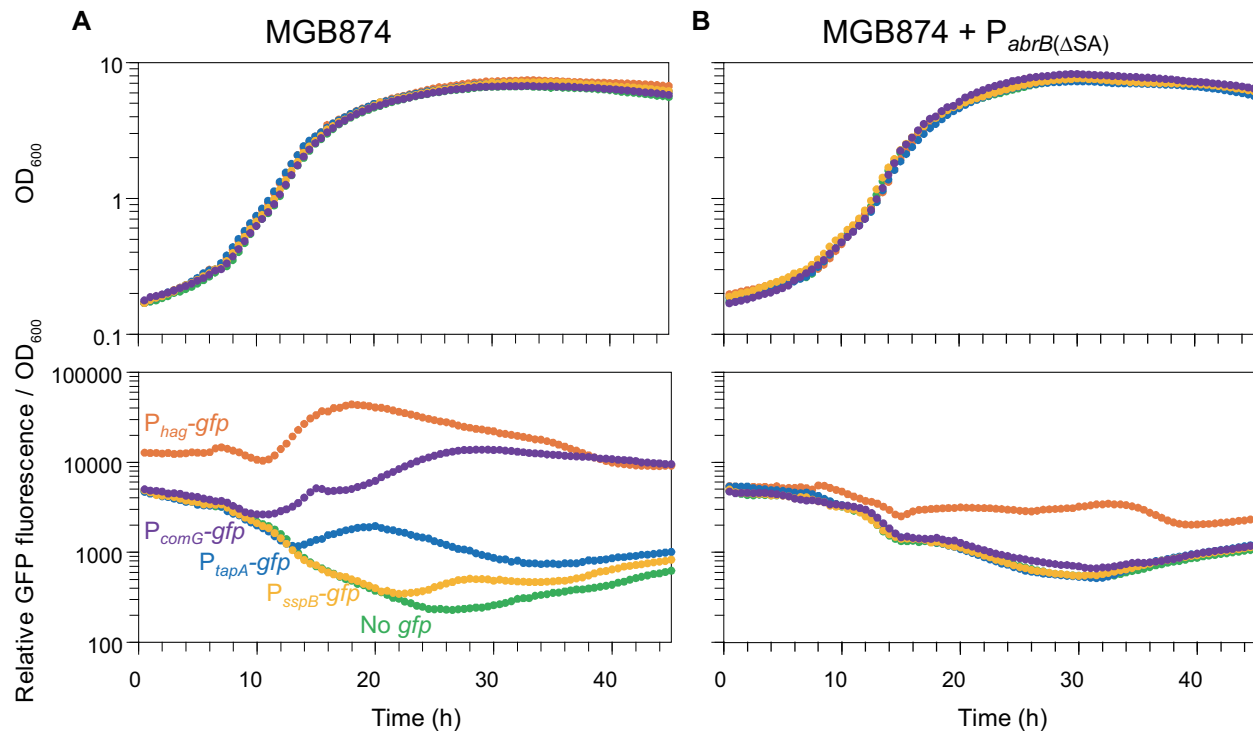


**Figure 4.** Effect of  $P_{abrB(\Delta SA)}$  on the activities of  $P_{hag}$ -gfp,  $P_{tapA}$ -gfp,  $P_{sspB}$ -gfp, and  $P_{comG}$ -gfp. (A) OA225 (MGB874 carrying  $P_{hag}$ -gfp, orange), OA226 (MGB874 carrying  $P_{tapA}$ -gfp, blue), OA227 (MGB874 carrying  $P_{sspB}$ -gfp, yellow), OA228 (MGB874 carrying  $P_{comG}$ -gfp, purple), and MGB874 (green) were grown in the minimal medium containing 20 g l<sup>-1</sup> glucose, and the fluorescence intensity and OD<sub>600</sub> were recorded every 30 min. (B) OA229 [MGB874 carrying  $P_{hag}$ -gfp,  $P_{abrB(\Delta SA)}$ , orange], OA230 [MGB874 carrying  $P_{tapA}$ -gfp,  $P_{abrB(\Delta SA)}$ , blue], OA231 [MGB874 carrying  $P_{sspB}$ -gfp,  $P_{abrB(\Delta SA)}$ , yellow], OA232 [MGB874 carrying  $P_{comG}$ -gfp,  $P_{abrB(\Delta SA)}$ , purple], and OA191 [MGB874 carrying  $P_{abrB(\Delta SA)}$ , green] were grown and the fluorescence intensity and OD<sub>600</sub> were recorded as in (A). (A color version of this figure appears in the online version of this article.)

the estimated flux distributions can explain the measured MIDs because the threshold of chi-squared test for goodness of fit was 118.8 (the number of independent data was 111, while the number of degrees of freedom of the reaction model was 16). The flux distributions of CMP are shown in Fig. 7A, and the associated 95% CIs are shown in Supplementary Table S6. The glycolytic flux was increased in the  $P_{abrB(\Delta SA)}$  strain. For example, in the glucose-6-phosphate isomerase reaction, the upstream step in glycolysis, the 95% CI was 3.8–4.5 mmol g-DCW<sup>-1</sup> h<sup>-1</sup> in the  $P_{abrB(\Delta SA)}$  strain and was 2.3–3.0 mmol g-DCW<sup>-1</sup> h<sup>-1</sup> in the MGB874 strain.

This change in glycolytic flux was consistent with that found for the transcription levels. Furthermore, the acetate overflow flux was increased in the  $P_{abrB(\Delta SA)}$  strain (Table 1), which is also consistent with the upregulation of *pta* and *ackA*, which are responsible for acetate overflow (Fig. 7A). In contrast, the fluxes of the PPP and TCA cycle of the  $P_{abrB(\Delta SA)}$  strain were lower than those of the MGB874 strain. The expression levels of the genes for these pathways were higher in the  $P_{abrB(\Delta SA)}$  strain than in the parent strain, but increases were statistically not significant. These differences explain the greater flux toward glycolysis and acetate overflow than the PPP and TCA cycle.

### 3.6. $P_{abrB(\Delta SA)}$ mutation increases the transcription of genes involved in the biosynthesis of purine/pyrimidine nucleotides and amino acids in MGB874

The functional enrichment analysis also detected enrichment of the pyrimidine and purine metabolism metabolisms ( $P = 3.3 \times 10^{-6}$  and  $1.6 \times 10^{-5}$ , respectively) and of the alanine, aspartate, and glutamate

metabolism ( $P = 5.2 \times 10^{-5}$ ). Thus, we further compared the transcriptional profiles of genes involved in biosynthesis of amino acids and purine/pyrimidine nucleotides using scatter plots (Fig. 8A–D), statistical evaluation of the overall transcriptional change (Fig. 8E–G), and volcano plots (Fig. 8H). The overall tendencies were similar to those found for the transcriptional changes of CMP genes. In all cases, the overall transcription levels were significantly lower in MGB874 than in OA105, and 80%, 83%, and 30% of the genes for biosynthesis of purines, pyrimidines, and amino acids, respectively, were significantly downregulated in MGB874 (Supplementary Table S3). Moreover, the introduction of  $P_{abrB(\Delta SA)}$  into MGB874 (strain OA191) restored the overall expression levels of these gene groups to the levels in OA105 (Fig. 8E–G) and significantly upregulated 85%, 67%, and 33% of the genes for biosynthesis of purines, pyrimidines, and amino acids, respectively (Fig. 8H and Supplementary Table S3).

### 3.7. $P_{abrB(\Delta SA)}$ mutation enhances $\gamma$ -PGA production

Although the MGB874 strain was unable to produce  $\gamma$ -PGA in MMOPS minimal medium, by placing the  $\gamma$ -PGA synthase genes (*pgsBCAE*) under the control of a strong promoter in the *amyE* region and deleting the genes from the original chromosome region, 2.2 g l<sup>-1</sup> of  $\gamma$ -PGA was produced in the minimal medium containing 50 g l<sup>-1</sup> glucose (Table 2). Additional introduction of the  $P_{abrB(\Delta SA)}$  mutation enhanced the production of  $\gamma$ -PGA to 4.1 g l<sup>-1</sup>, nearly doubling the yield. Considering that the OD<sub>600</sub> of the  $P_{abrB(\Delta SA)}$  strain increased by 2-fold, these results indicated that the ability to produce  $\gamma$ -PGA has been almost doubled due to the restoration of growth rate by the introduction



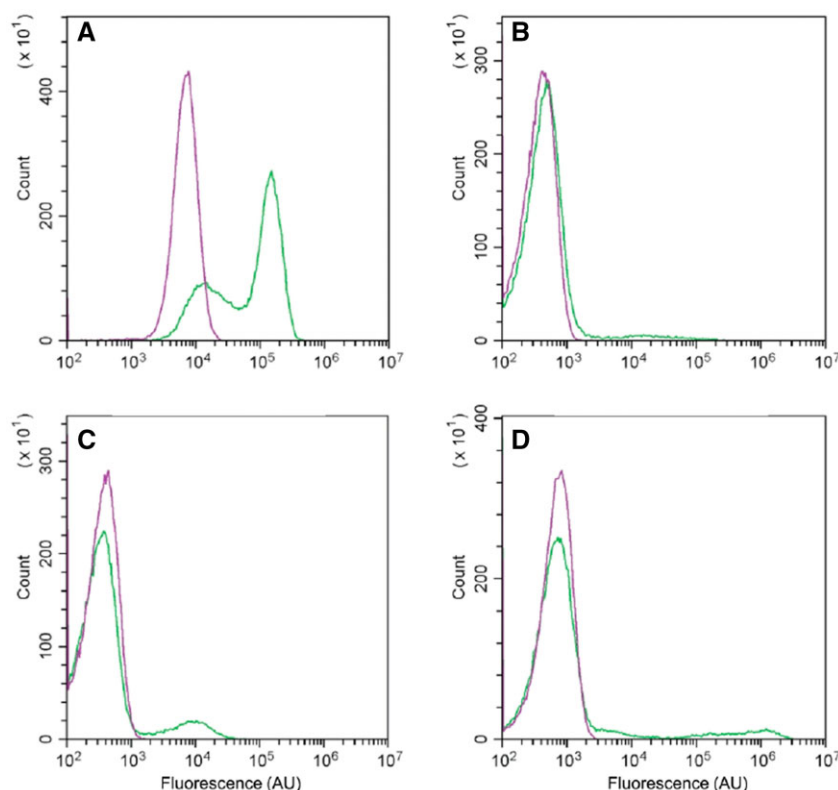


**Figure 5.** Flow cytometric analysis of the expression of  $P_{hag-gfp}$  (A),  $P_{tapA-gfp}$  (B),  $P_{sspB-gfp}$  (C), and  $P_{comGA-gfp}$  (D) in MGB874 (green line) and its  $P_{abrB(\Delta SA)}$ -derivative (purple line). Cells were cultured as described in the legend to Fig. 4 for 20 h (A and B) or 30 h. (A color version of this figure appears in the online version of this article.)

of  $P_{abrB(\Delta SA)}$ . Thus, through genome reduction and constitutive high expression of AbrB, we were able to construct a strain with drastically enhanced productivity of desired substance.

### 3.8. $P_{abrB(\Delta SA)}$ mutation enhances cellulase productivity in the wild-type strain

We predicted that silencing the AbrB regulon by the  $P_{abrB(\Delta SA)}$  mutation would reduce the cellular burden, as in the case of genome reduction, leading to enhanced bioproduction. Although the introduction of this mutation did not change the growth rates of the wild-type strain OA105 or the 168 strain (Fig. 2 and data not shown), cellulase production in the minimal medium containing  $50 \text{ g l}^{-1}$  glucose, as determined based on the activities per culture volume or further normalized by  $\text{OD}_{600}$ , increased by 1.7- and 2.0-fold, respectively, when the  $P_{abrB(\Delta SA)}$  mutation was introduced in the wild-type strain 168 (Table 3). This result indicated that the mutant strain has approximately double the ability to produce cellulase. Consistently, transcriptome analysis of OA105 and its  $P_{abrB(\Delta SA)}$ -introduced derivative revealed statistically significant global transcriptional repression of AbrB-regulated genes in the  $P_{abrB(\Delta SA)}$ -introduced OA190 strain (Fig. 6D and E), with 56% of the genes being downregulated (Supplementary Table S3). Although there was no apparent overall or statistically significant transcriptional change of genes for the CMP or biosynthesis of pyrimidine nucleotides (Figs 6D, F, 8D, and G), significantly increased transcription was detected for genes involved in the biosynthesis of amino acids and purine nucleotides (Fig. 8E and F), which may have contributed to increased metabolite productivity.

## 4. Discussion

The soil-dwelling bacterium *B. subtilis* has evolved sophisticated regulatory networks to differentiate cells into distinct subpopulations present in multicellular communities.<sup>12,44,45</sup> During the exponential growth phase, the genes required for this cell differentiation are strictly repressed by AbrB.<sup>12–14</sup> Under laboratory conditions, such genes are strictly repressed in a rich medium. However, in minimal medium, we found that the *sdpA* promoter was induced in the exponential growth phase (Fig. 3), indicating that the repression by AbrB was relieved, leading to induction of the AbrB-regulated genes, which may burden the cells. In the genome-reduced strain MGB874, AbrB-regulated genes were unexpectedly expressed more highly than those in the wild-type strain when grown in minimal medium.

Genome reduction is intended to remove redundant or less important genes with detrimental risk to reduce the aforementioned cellular burden. In fact, the MGB874 strain shows increased productivity of cellulase and protease<sup>3,4</sup>; however, this comes at a cost of a negative phenotype exhibiting slower growth on minimal medium. In this strain, 155 of the 249 genes regulated by AbrB remained, and this insufficient suppression by AbrB resulted in the significant upregulation of 21% of the 155 genes in the minimal medium compared with their expression in the wild-type strain OA105. Since the transcription level of *abrB* did not change in MGB874 (Supplementary Table S3), this partial derepression of AbrB-regulated genes could be caused by other mechanisms such as reduction of AbrB activity through AbrB phosphorylation by serine/threonine kinases<sup>46</sup> or inhibition of AbrB activity through AbbA binding.<sup>47</sup> Although it was not clear if one or both of these mechanisms is the primary cause, or if

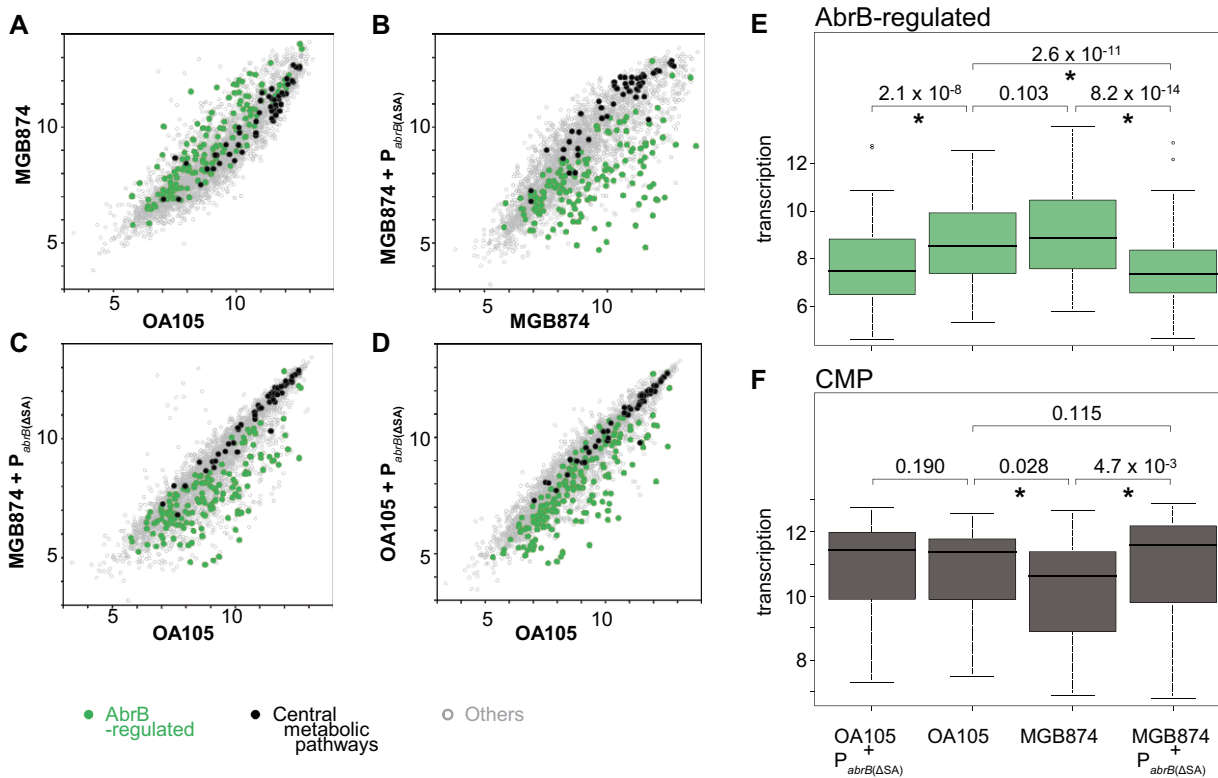


**Figure 6.** Comparison of the transcriptome profiles of AbrB-regulated and CMP genes between OA105 and MGB874 with or without the  $P_{abrB(\Delta SA)}$  mutation. (A–D) Scatter plots (log<sub>2</sub> scale) of the transcriptional signals of each gene. AbrB-regulated (green) and CMP (black) genes are shown as colored dots. The other genes are shown as gray dots. (A) Scatter plots of OA105 and MGB874 cells. (B) Scatter plots of the MGB874 and MGB874 containing  $P_{abrB(\Delta SA)}$  strains (OA191). (C) Scatter plots of the OA105 and MGB874 containing  $P_{abrB(\Delta SA)}$  strains (OA191). (D) Scatter plots of the OA105 and OA105 containing  $P_{abrB(\Delta SA)}$  strains (OA190). (E–F) Box plots (log<sub>2</sub> scale) of transcription levels of AbrB-regulated and CMP genes in the OA105, MGB874, OA105 containing  $P_{abrB(\Delta SA)}$  (OA190), and MGB874 containing  $P_{abrB(\Delta SA)}$  (OA191) strains. Whiskers show minimum and maximum values, boxes represent the 25–75% data ranges, and horizontal lines within boxes are medians.  $P$  values calculated with one-sided Mann–Whitney U-test are shown.  $P$  values < 0.05 were considered to be significantly different (marked with an asterisk). (A color version of this figure appears in the online version of this article.)

there are other reasons, we hypothesized that upregulation of some AbrB-regulated genes in MGB874 was the cause of the slower growth. In support of this hypothesis, introduction of the  $P_{abrB(\Delta SA)}$  mutation, which enables constitutive high expression of AbrB, restored the slow-growth phenotype in MGB874.

In the  $P_{abrB(\Delta SA)}$  strain, in addition to repression of the AbrB-regulated genes, the expression of genes involved in CMP and in the biosynthesis of amino acids and purine/pyrimidine nucleotides was restored to wild-type levels which was accompanied by an increase in the metabolic flux of glycolysis. These results suggested that in MGB874, the upregulation of AbrB-regulated genes may burden the cells and lead to the downregulation of genes for these metabolic pathways. Although it is unclear whether the effect of the upregulation of AbrB-repressed genes is direct or not, it is responsible for the slow-growth phenotype of MGB874 as this deleterious phenotype was ameliorated by introducing the  $P_{abrB(\Delta SA)}$  mutation.

In the  $P_{abrB(\Delta SA)}$  strain,  $P_{tapA-gfp}$ , the promoter directly repressed by AbrB, along with the promoters indirectly repressed by AbrB, namely  $P_{hag-gfp}$ ,  $P_{sspB-gfp}$ , and  $P_{comG-gfp}$ , were repressed in minimal medium. This result indicates that the transcriptional network centered on AbrB was also tightly repressed in this strain, leading to the inhibition of cell differentiation to several cell types, which was observed in the parent MGB874. As such differentiation occurred in only a small fraction of cell population, it is unknown how much this inhibition contributed to the transcriptomic and metabolic

changes that occurred in the  $P_{abrB(\Delta SA)}$ -introduced strain. However, maintaining the cell population in an undifferentiated state may be important to improve its bioproduktivity. In fact, the production of  $\gamma$ -PGA, which is produced from glucose via CMP in minimal medium containing glucose as the sole carbon source, was remarkably improved by introducing the  $P_{abrB(\Delta SA)}$  mutation (Table 2).

The bimodal expression pattern detected for  $P_{hag-gfp}$  was previously reported in the undomesticated wild-type strain NCBI3610 using  $P_{hag-yfp}$ .<sup>48</sup> In this case, only the higher intensity peak was observed in its deletion mutant of  $flgN$  ( $yvyG$ ), which encodes a chaperone protein essential for flagellar filament polymerization, and this shift was likely due to a change in regulation by the anti-sigma factor for SigD, FlgM. In contrast, we found that in the  $P_{abrB(\Delta SA)}$ -introduced MGB874 strain, only the lower intensity peak was observed. In addition, the transcription levels of  $flgN$ ,  $flgM$ , and  $sigD$  were not changed in the  $P_{abrB(\Delta SA)}$  strain, indicating that in the strain,  $P_{hag-gfp}$  was repressed in a manner independent of these genes. It seems that ScoC is also not involved in the repression of  $P_{hag-gfp}$ ,<sup>49</sup> because  $scoC$  expression was not upregulated in the  $P_{abrB(\Delta SA)}$  strain. Thus, it is unclear how constitutive overexpression of AbrB represses  $P_{hag}$ , and further studies are needed to elucidate the mechanism.

Regarding cellulase production, it was reported that cellulase accumulated at a similar rate for up to 20 h to >2,000 U l<sup>-1</sup> in both the 168 and MGB874 strains; however, while the production was arrested at this point in the 168 strain, it continued in the MGB874



**Table 1.** Growth rate and glucose uptake, acetate production, and succinate production of MGB874 and its  $P_{abrB}(\Delta SA)$  strains

<sup>a</sup>The growth characteristics of the indicated strains in the minimal medium containing 10 g l<sup>-1</sup> glucose over 5–6 h.  
<sup>b</sup>The data are presented as the mean  $\pm$  SD ( $n = 3$ ).

tight repression of the transcriptional network centered on AbrB by the *P<sub>abrB</sub>(ASA)* mutation would reduce the cellular burden, similar to the effect of genome reduction in MGB874, leading to the enhancement of bioproduction, even in wild-type cells.

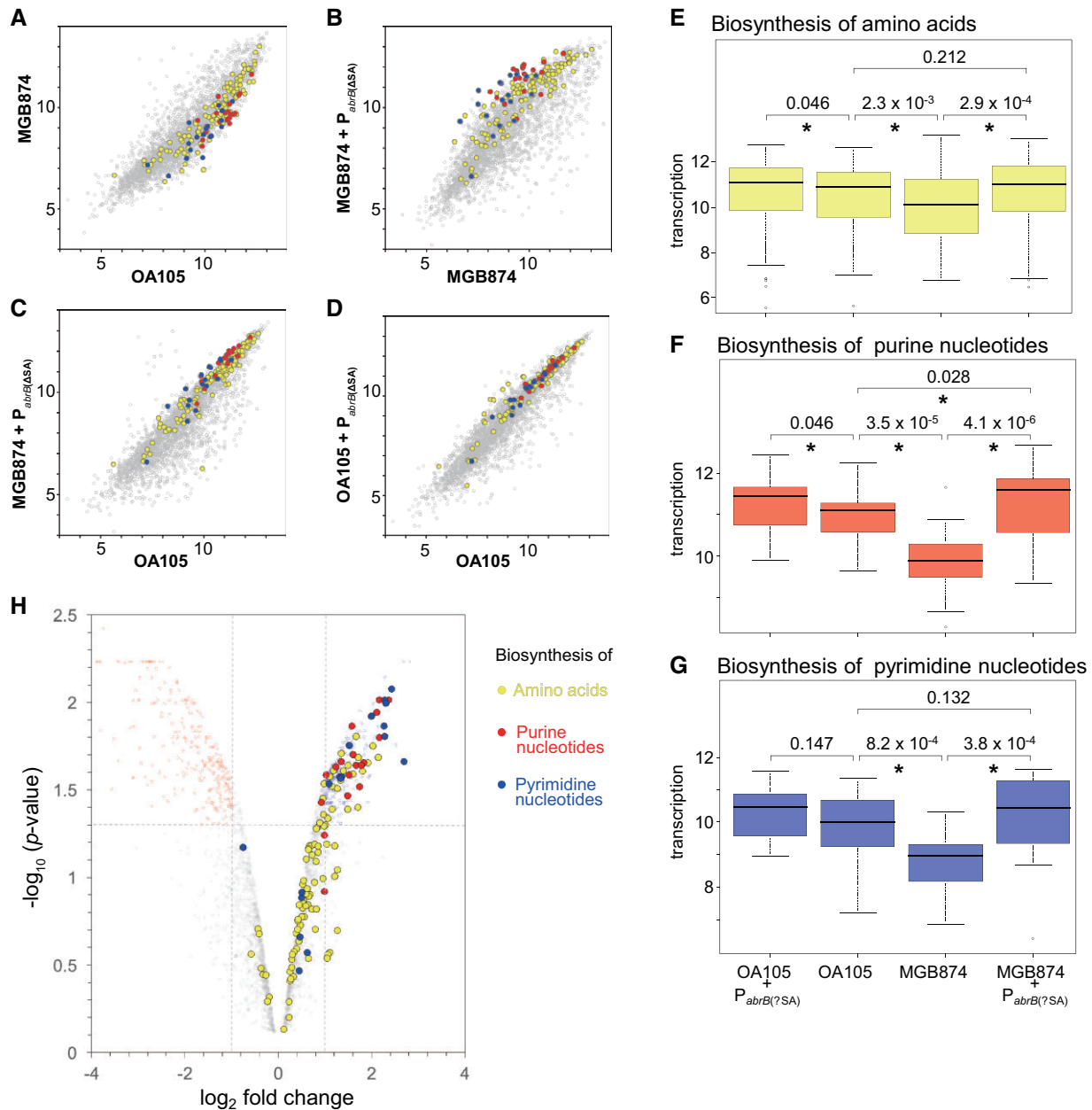


**Figure 8.** Comparison of transcriptome profiles of genes involved in the biosynthesis of amino acids and purine/pyrimidine nucleotides. (A–D) Scatter plots ( $\log_2$  scale) of the transcriptional signals of each gene. Genes involved in the biosynthesis of amino acids and purine and pyrimidine nucleotides are indicated by yellow, red, and blue dots, respectively (CMP genes are included in ‘other genes’). (E–G) Box plots ( $\log_2$  scale) of transcription levels of genes involved in the biosynthesis of amino acids and purine and pyrimidine nucleotides. Details are the same as described in the legend for Fig. 6E–F. (H) Volcano plot analysis of the gene expression levels between MGB874 and OA191. The genes involved in the biosynthesis of amino acids and purine and pyrimidine nucleotides are colored as in (A–D).

**Table 2.**  $\gamma$ -PGA production in MGB874 and its  $P_{abrB(\Delta SA)}$  derivative

Strain	$\gamma$ -PGA production <sup>a</sup>	
	U l <sup>-1</sup>	U l <sup>-1</sup> OD <sub>600</sub> <sup>-1</sup>
A-278 (MGB874: $\gamma$ -PGA production genes) <sup>b</sup>	2.2 ± 0.1 (100)	0.25 ± 0.014 (100)
A-306 [MGB874: $\gamma$ -PGA production genes, $P_{abrB(\Delta SA)}$ ]	4.1 ± 1.4 (189)	0.45 ± 0.032 (182)
P-value	0.042	9.8 × 10 <sup>-4</sup>

<sup>a</sup>The data are presented as means ± SD ( $n = 3$ ). Relative  $\gamma$ -PGA production compared with that of A-278 are indicated in parentheses.

<sup>b</sup> $P_{pmo-pgsBCAE}$  (to overexpress the  $\gamma$ -PGA synthase genes) and  $tufA-pgdS$  (to overexpress a  $\gamma$ -glutamyl hydrolase gene to decrease culture viscosity and increase  $\gamma$ -PGA productivity) are inserted in the *amyE* region. The *pgsBCAE-pgdS* sequence in the original chromosome region has been deleted.

Table 3. Cellulase activities

Strain	Cellulase activities <sup>a</sup>	
	U l <sup>-1</sup>	U l <sup>-1</sup> OD <sub>600</sub> <sup>-1</sup>
168 (pHYS237)	2787 ± 136 (100)	107 ± 17 (100)
168: P <sub>abrB(ΔSA)</sub> (pHYS237) <sup>b</sup>	4691 ± 84 (168)	217 ± 20 (203)
P-value	3.3 × 10 <sup>-5</sup>	1.0 × 10 <sup>-3</sup>

<sup>a</sup>The data are presented as the mean ± SD (*n* = 3). Relative cellulase activities compared with that of 168 (pHYS237) are indicated in parentheses.

<sup>b</sup>A-395 strain, a 168-derivative carrying the P<sub>abrB(ΔSA)</sub> mutation.

Based on previous findings for the wild-type strain JH642 with the *spo0A*-null mutation (*spo0A12*)<sup>17</sup> (see Introduction for details), we initially expected that the increase in AbrB level would also increase the growth rates of the wild-type strains 168 and OA105 in minimal medium; however, the growth rate was not further increased. The downregulation of genes involved in CMP and the biosynthesis of amino acids and purine/pyrimidine nucleotides, which contributed to the decreased growth rate of MGB874, was not observed in the OA105 strain. Thus, the increase in AbrB level did not further increase the growth rate. Strains JH642 and 168 strains have 1,734 single-nucleotide polymorphisms (SNPs) in the 71-kb hyper-variable region along with 35 SNPs distributed over the rest of the genome.<sup>50</sup> These differences may be responsible for the reduced growth of JH642 in minimal media, and the increased AbrB level due to the *spo0A12* mutation may have restored the growth rate of JH642.

In summary, we have demonstrated that tight repression of a set of genes regulated by a global transcriptional regulator is an effective strategy for reducing the burden on cells to achieve higher bioproduction. This is probably effective in not only genome-reduced strains, in which a large number of unnecessary genes remain and/or the transcriptional network may be unexpectedly disturbed by genome engineering but also wild-type strains in which the transcriptional network may be disturbed under unnatural conditions for laboratory work or metabolite production. This is the first report of a method to improve the bioproduktivity of genome-reduced strains by modifying a global transcription network, which can be developed as a key technology in the future not only *B. subtilis* and related species but also other bacteria with a mechanism to globally represses unwanted gene expression, such as the H-NS-mediated gene silencing in *E. coli*.<sup>51</sup>

Acknowledgements

This work was supported by the Advanced Low Carbon Technology Research and Development Program of the Japan Science and Technology Agency (J.S.T.). S.I. was supported by JSPS KAKENHI (Grant-in-Aid for Challenging Research [Pioneering]) Grant Number JP18H05360. We thank Katsuya Ozaki (Kao Corp.) and Hiroshi Hagihara (Kao Corp.) for their helpful discussions. We also thank our anonymous reviewers and the editor Katsumi Isono for valuable advice.

Conflict of interest None declared.

Supplementary data

Supplementary data are available at DNARES online.

References

1. Juhas, M., Reuß, D.R., Zhu, B. and Commichau, F.M. 2014, *Bacillus subtilis* and *Escherichia coli* essential genes and minimal cell factories after one decade of genome engineering, *Microbiology (Reading)*, **160**, 2341–51.

2. Landon, S., Rees-Garbutt, J., Marucci, L. and Grierson, C. 2019, Genome-driven cell engineering review: *in vivo* and *in silico* metabolic and genome engineering, *Essays Biochem.*, **63**, 267–84.

3. Morimoto, T., Kadoya, R., Endo, K., et al. 2008, Enhanced recombinant protein productivity by genome reduction in *Bacillus subtilis*, *DNA Res.*, **15**, 73–81.

4. Manabe, K., Kageyama, Y., Morimoto, T., et al. 2013, Improved production of secreted heterologous enzyme in *Bacillus subtilis* strain MGB874 via modification of glutamate metabolism and growth conditions, *Microb. Cell Fact.*, **12**, 18.

5. Aguilar Suárez, R., Stülke, J. and van Dijk, J.M. 2019, Less is more: toward a genome-reduced *Bacillus* cell factory for “difficult Proteins”, *ACS Synth. Biol.*, **8**, 99–108.

6. van Tilburg, A.Y., van Heel, A.J., Stülke, J., de Kok, N.A.W., Rueff, A.-S. and Kuipers, O.P. 2020, Mini *Bacillus* PG10 as a convenient and effective production host for lantibiotics, *ACS Synth. Biol.*, **9**, 1833–42.

7. Hirokawa, Y., Kawano, H., Tanaka-Masuda, K., et al. 2013, Genetic manipulations restored the growth fitness of reduced-genome *Escherichia coli*, *J. Biosci. Bioeng.*, **116**, 52–8.

8. Ara, K., Ozaki, K., Nakamura, K., Yamane, K., Sekiguchi, J. and Ogasawara, N. 2007, *Bacillus* minimum genome factory: effective utilization of microbial genome information, *Biotechnol. Appl. Biochem.*, **46**, 169–78.

9. Hashimoto, M., Ichimura, T., Mizoguchi, H., et al. 2005, Cell size and nucleoid organization of engineered *Escherichia coli* cells with a reduced genome, *Mol. Microbiol.*, **55**, 137–49.

10. Reuß, D.R., Altenbuchner, J., Mäder, U., et al. 2017, Large-scale reduction of the *Bacillus subtilis* genome: consequences for the transcriptional network, resource allocation, and metabolism, *Genome Res.*, **27**, 289–99.

11. Michalik, S., Reder, A., Richts, B. R., et al. 2021, The *Bacillus subtilis* minimal genome compendium, *ACS Synth. Biol.*, **10**, 2767–71.

12. López, D., Vlamakis, H. and Kolter, R. 2009, Generation of multiple cell types in *Bacillus subtilis*, *FEMS Microbiol. Rev.*, **33**, 152–63.

13. Chumsakul, O., Takahashi, H., Oshima, T., et al. 2011, Genome-wide binding profiles of the *Bacillus subtilis* transition state regulator AbrB and its homolog Abh reveals their interactive role in transcriptional regulation, *Nucleic Acids Res.*, **39**, 414–28.

14. Chumsakul, O., Nakamura, K., Kurata, T., et al. 2013, High-resolution mapping of *in vivo* genomic transcription factor binding sites using *in situ* DNase I footprinting and ChIP-seq, *DNA Res.*, **20**, 325–38.

15. Chai, Y., Chu, F., Kolter, R. and Losick, R. 2008, Bistability and biofilm formation in *Bacillus subtilis*, *Mol. Microbiol.*, **67**, 254–63.

16. Strauch, M., Webb, V., Spiegelman, G. and Hoch, J.A. 1990, The Spo0A protein of *Bacillus subtilis* is a repressor of the *abrB* gene, *Proc. Natl. Acad. Sci. U. S. A.*, **87**, 1801–5.

17. Kudoh, J., Ikeuchi, T. and Kurahashi, K. 1985, Nucleotide sequences of the sporulation gene *spo0A* and its mutant genes of *Bacillus subtilis*, *Proc. Natl. Acad. Sci. U. S. A.*, **82**, 2665–8.

18. Fisher, S.H., Strauch, M.A., Atkinson, M.R. and Wray, L.V. Jr, 1994, Modulation of *Bacillus subtilis* catabolite repression by transition state regulatory protein AbrB, *J. Bacteriol.*, **176**, 1903–12.

19. Park, J.H., Lee, K.H., Kim, T.Y. and Lee, S.Y. 2007, Metabolic engineering of *Escherichia coli* for the production of L-valine based on transcriptome analysis and *in silico* gene knockout simulation, *Proc. Natl. Acad. Sci. U. S. A.*, **104**, 7797–802.

20. Gao, X., Yang, X., Li, J., Zhang, Y., Chen, P. and Lin, Z. 2018, Engineered global regulator H-NS improves the acid tolerance of *E. coli*, *Microb. Cell Fact.*, **17**, 1–13.

21. Ali Azam, T., Iwata, A., Nishimura, A., Ueda, S. and Ishihama, A. 1999, Growth phase-dependent variation in protein composition of the *Escherichia coli* nucleoid, *J. Bacteriol.*, **181**, 6361–70.



22. Wang, W., Li, G.-W., Chen, C., Xie, X.S. and Zhuang, X. 2011, Chromosome organization by a nucleoid-associated protein in live bacteria, *Science*, **333**, 1445–9.
23. Rösch, T.C., Oviedo-Bocanegra, L.M., Fritz, G. and Graumann, P.L. 2018, SMTracker: a tool for quantitative analysis, exploration and visualization of single-molecule tracking data reveals highly dynamic binding of *B. subtilis* global repressor AbrB throughout the genome, *Sci. Rep.*, **8**, 1–12.
24. Higashi, K., Tobe, T., Kanai, A., et al. 2016, H-NS facilitates sequence diversification of horizontally transferred DNAs during their integration in host chromosomes, *PLoS Genet.*, **12**, e1005796.
25. Toya, Y., Hirasawa, T., Ishikawa, S., et al. 2015, Enhanced dipicolinic acid production during the stationary phase in *Bacillus subtilis* by blocking acetoin synthesis, *Biosci. Biotechnol. Biochem.*, **79**, 2073–80.
26. Lei, Y., Oshima, T., Ogasawara, N. and Ishikawa, S. 2013, Functional analysis of the protein Veg, which stimulates biofilm formation in *Bacillus subtilis*, *J. Bacteriol.*, **195**, 1697–705.
27. Mori, K., Verrone, V., Amatsu, R., et al. 2021, Assessment of *Bacillus subtilis* plasmid pLS20 conjugation in the absence of quorum sensing repression, *Microorganisms*, **9**, 1931.
28. Oshima, T., Ishikawa, S., Kurokawa, K., Aiba, H. and Ogasawara, N. 2006, *Escherichia coli* histone-like protein H-NS preferentially binds to horizontally acquired DNA in association with RNA polymerase, *DNA Res.*, **13**, 141–53.
29. Kusuya, Y., Kurokawa, K., Ishikawa, S., Ogasawara, N. and Oshima, T. 2011, Transcription factor GreA contributes to resolving promoter-proximal pausing of RNA polymerase in *Bacillus subtilis* cells, *J. Bacteriol.*, **193**, 3090–9.
30. Pedreira, T., Elfmann, C. and Stülke, J. 2021, The current state of SubtiWiki, the database for the model organism *Bacillus subtilis*, *Nucleic Acids Res.*, **50**, D875–82.
31. Kanehisa, M., Furumichi, M., Sato, Y., Ishiguro-Watanabe, M. and Tanabe, M. 2021, KEGG: integrating viruses and cellular organisms, *Nucleic Acids Res.*, **49**, D545–51.
32. Zhou, G., Soufan, O., Ewald, J., Hancock, R.E., Basu, N. and Xia, J. 2019, NetworkAnalyst 3.0: a visual analytics platform for comprehensive gene expression profiling and meta-analysis, *Nucleic Acids Res.*, **47**, W234–41.
33. Ritchie, M.E., Phipson, B., Wu, D., et al. 2015, *limma* powers differential expression analyses for RNA-sequencing and microarray studies, *Nucleic Acids Res.*, **43**, e47.
34. Usui, Y., Hirasawa, T., Furusawa, C., et al. 2012, Investigating the effects of perturbations to *pgi* and *eno* gene expression on central carbon metabolism in *Escherichia coli* using <sup>13</sup>C metabolic flux analysis, *Microb. Cell Fact.*, **11**, 1–16.
35. Matsuda, F., Toya, Y. and Shimizu, H. 2017, Learning from quantitative data to understand central carbon metabolism, *Biotechnol. Adv.*, **35**, 971–80.
36. Antoniewicz, M.R., Kelleher, J.K. and Stephanopoulos, G. 2007, Elementary metabolite units (EMU): a novel framework for modeling isotopic distributions, *Metab. Eng.*, **9**, 68–86.
37. Sauer, U., Hatzimanikatis, V., Hohmann, H.P., Manneberg, M., van Loon, A.P. and Bailey, J.E. 1996, Physiology and metabolic fluxes of wild-type and riboflavin-producing *Bacillus subtilis*, *Appl. Environ. Microbiol.*, **62**, 3687–96.
38. Antoniewicz, M.R., Kelleher, J.K. and Stephanopoulos, G. 2006, Determination of confidence intervals of metabolic fluxes estimated from stable isotope measurements, *Metab. Eng.*, **8**, 324–37.
39. Kajihata, S., Furusawa, C., Matsuda, F. and Shimizu, H. 2014, OpenMebius: an open source software for isotopically nonstationary <sup>13</sup>C-based metabolic flux analysis, *Biomed Res. Int.*, **2014**, 627014.
40. Sawada, K., Araki, H., Takimura, Y., et al. 2018, Poly-L-gamma-glutamic acid production by recombinant *Bacillus subtilis* without *pgsA* gene, *AMB Expr.*, **8**, 1–11.
41. Hakamada, Y., Hatada, Y., Koike, K., et al. 2000, Deduced amino acid sequence and possible catalytic residues of a thermostable, alkaline cellulase from an alkaliphilic *Bacillus* strain, *Biosci. Biotechnol. Biochem.*, **64**, 2281–9.
42. Gaidenko, T.A. and Price, C.W. 1998, General stress transcription factor  $\sigma^B$  and sporulation transcription factor  $\sigma^H$  each contribute to survival of *Bacillus subtilis* under extreme growth conditions, *J. Bacteriol.*, **180**, 3730–3.
43. Mendez, M.B., Orsaria, L.M., Philippe, V., Pedrido, M.E. and Grau, R.R. 2004, Novel roles of the master transcription factors Spo0A and  $\sigma^B$  for survival and sporulation of *Bacillus subtilis* at low growth temperature, *J. Bacteriol.*, **186**, 989–1000.
44. Vlamakis, H., Chai, Y., Beauregard, P., Losick, R. and Kolter, R. 2013, Sticking together: building a biofilm the *Bacillus subtilis* way, *Nat. Rev. Microbiol.*, **11**, 157–68.
45. Arnaouteli, S., Bamford, N.C., Stanley-Wall, N.R. and Kovacs, A.T. 2021, *Bacillus subtilis* biofilm formation and social interactions, *Nat. Rev. Microbiol.*, **19**, 600–14.
46. Kobir, A., Poncet, S., Bidnenko, V., et al. 2014, Phosphorylation of *Bacillus subtilis* gene regulator AbrB modulates its DNA-binding properties, *Mol. Microbiol.*, **92**, 1129–41.
47. Banse, A.V., Chastanet, A., Rahn-Lee, L., Hobbs, E.C. and Losick, R. 2008, Parallel pathways of repression and antirepression governing the transition to stationary phase in *Bacillus subtilis*, *Proc. Natl. Acad. Sci. U. S. A.*, **105**, 15547–52.
48. Cairns, L.S., Marlow, V.L., Kiley, T.B., et al. 2014, FlgN is required for flagellum-based motility by *Bacillus subtilis*, *J. Bacteriol.*, **196**, 2216–26.
49. Kodgire, P. and Rao, K.K. 2009, *bag* expression in *Bacillus subtilis* is both negatively and positively regulated by ScoC, *Microbiology (Reading)*, **155**, 142–9.
50. Smith, J.L., Goldberg, J.M. and Grossman, A.D. 2014, Complete genome sequences of *Bacillus subtilis* subsp. *subtilis* laboratory strains JH642 (AG174) and AG1839, *Genome Announc.*, **2**, e00663-14.
51. Lamberte, L.E., Baniulyte, G., Singh, S.S., et al. 2017, Horizontally acquired AT-rich genes in *Escherichia coli* cause toxicity by sequestering RNA polymerase, *Nat. Microbiol.*, **2**, 16249.